Accepted Manuscript

RENEWAL MODELS OF SEISMIC RECURRENCE APPLIED TO PALEOSEISMOLOGICAL AND HISTORICAL OBSERVATIONS

I. Mosca[1], R. Console[2,3] and G. D'Addezio[2]

[1]Department of Earth and Environmental Sciences, LMU, Munich, Germany

[2]Istituto Nazionale di Geofisica e Vulcanologia, Rome, Italy

[3]Centro di Geomorfologia Integrata per l'Area del Mediterraneo, Potenza, Italy

Abstract

Because paleoseismology can extend the record of earthquakes back in time up to several millennia, it represents an opportunity to study how earthquakes recur through time and thus to provide innovative contributions to seismic hazard assessment. Based on a database of recurrence from paleoseismology we collected 19 sequences with 5 up to 14 dated events on a single fault. By using the age of the paleoearthquakes, with their associated uncertainty, and the historical earthquakes, we tested the null hypothesis that the observed inter-event times come from a uniform random distribution (Poisson model). We used the concept of likelihood for a specific sequence of events under a given occurrence model. The difference *dlnL* of the likelihoods estimated under two hypotheses gives an indication of which between the two hypotheses fits better the observations. To take into account the uncertainties, we used a Monte Carlo procedure computing the average and the standard deviation of *dlnL* for 1000 inter-event sets by choosing the occurrence time

of each event within the limits of uncertainty and estimating the probability that a value equal to or larger than a observed *dlnL* comes by chance from a Poisson distribution of inter-event times. These tests were carried out for the Log-normal, Gamma, Weibull, Double-exponential and Brownian Passage Time (BPT) distributions. Our results show that a renewal model, associated with a time dependent hazard, and some kind of predictability of the next large earthquake on a fault is significantly better than a plain time-independent Poisson model only for four, out of the 19 sites examined in this study. The lack of regularity in the earthquake occurrence for more than 30% of the examined faults can be explained either by the large uncertainties in the estimate of paleoseismological occurrence times or by physical interaction between neighbouring faults.

In the last decades the use of probabilistic, long-term time-dependent models of earthquake occurrence has grown up in the context of seismic hazard analysis. The basic idea for time-dependent models is universally known as the elastic rebound theory, initially proposed by Reid (1910) in the context of his study of the great San Francisco, 1906 earthquake: stresses which cause earthquakes are slowly built up by plate movements until the stress or deformation energy reaches a critical value, at which a rupture occurs. Later on, in connection with the development of the plate tectonics theory, this idea has been worked out by Mogi (1968) in its definition of

the seismic gap of the first kind. A seismic gap of the first kind is a segment of plate boundary, for which the time elapsed since its latest rupture is significantly long relatively to that of the neighbouring segments. According to a very popular and intuitive view, a seismic gap is likely to rupture again generating a large earthquake in the near future.

An extension of the seismic gap hypothesis can be recognized in the characteristic earthquake model (Schwartz and Coppersmith, 1984; Wesnousky, 1994). According to this model, strong earthquakes have a general inclination to repeat themselves along the same fault segment or plate boundary. The occurrence of a characteristic earthquake ruptures the entire segment and relieves tectonic stress within the segment. Therefore, the characteristic earthquake hypothesis cannot be taken independently of its implications on the time occurrence of earthquakes. In fact, if one assumes a constant average slip rate between two plates along their boundary, and a fairly constant slip and stress drop released by each characteristic earthquake on a fault, the regularity of the inter-event time is just a simple physical consequence. According to this hypothesis, the earthquake hazard is small immediately following the previous large earthquake and increases with time since the latest event on a certain fault or plate boundary. Hence, the earthquake occurrence can be regarded as a quasi-periodic process (McCann *et al*., 1979; Shimazaki and Nakata, 1980; Nishenko and Buland, 1987).

The controversy whether quasi-periodic or uniform inter-event time distributions apply to individual faults has been going on many years, and the choice affects not only earthquake probabilities and seismic hazard calculations, but also our understanding of the physics of earthquakes. This debate was partly developed through discussions by Nishenko and Sykes (1993), Jackson and Kagan (1993), Kagan and Jackson (1991, 1995), and Rong et al. (2003). The controversy did not have a clear conclusion and is ongoing.

Most recently, in the debate on the preference between a characteristic earthquake hypothesis and a simpler time-independent hypothesis, Parsons and Geist (2009) applied a simulator-based model. Their simulations showed that the Gutenberg-Richter distribution can be used as a model for earthquake occurrence on sub-segments of different size on individual faults in probabilistic earthquake forecasting.

In this study, we assume, as a working hypothesis, the characteristic earthquake model, and its periodicity. In order to assess the suitability of this hypothesis for its possible application to seismic forecasting, a probabilistic approach is used for comparison with a null hypothesis. In formulating this hypothesis we disregard any possible implication deriving from the geometry and other physical parameters of the earthquake sources. Earthquake occurrence is simply regarded as a point process, and the inter-event time is modelled by its probability density function

(*pdf*). In this respect, the null hypothesis is represented by an earthquake process without memory (described by a uniform Poisson process). For a uniform Poisson model, whose *pdf* is a negative exponential function, only one parameter, the inter-event time, is necessary for a complete description (Appendix A.1). Conversely, the gap hypothesis needs a more complicated model (i.e., the renewal models) whose *pdf* contains a further free parameter, affecting the shape of the distribution in terms of its periodicity. Typically, the *pdf* for a renewal model exhibits a maximum for inter-event times close to its expected recurrence time.

This work is aimed at assessing whether a collection of available occurrence times for sequences of strong earthquake in different areas of the world allows the test of the characteristic earthquake hypothesis described by the most popular renewal models, against a plain time-independent Poisson hypothesis. In this respect, this work can be considered a development of the paper published by Console *et al*., (2002). Assuming the Poisson hypothesis, their method was based on the comparison of the coefficient of variation observed for real seismic sequences with the distribution of the same parameter computed from a large number of simulations. In this case the comparison is based on the likelihood function computed for the real and simulated sequences.

1. METHOD

Any earthquake forecasting hypothesis should be objectively and unequivocally formulated so as to allow its validation through a stochastic procedure (Console, 2001). In the very popular Bayesian approach two hypotheses are compared: the first represents a commonly accepted conventional hypothesis (the null hypothesis), considered as a reference model, and the second is an alternative hypothesis. None of the hypothesis is claimed to be true, but any of them can be rejected with a given confidence level if its likelihood resulting from a set of observations is lower than a certain value.

In our study, as in many others of the past (e.g. see Kagan and Jackson, 1996; Console, 2001; Luen and Stark, 2008; Console et al., 2010), the reference model (the null hypothesis) of earthquake occurrence is the exponential distribution of the inter-event times in the continuous domain, also known as the Poisson model. The alternative models belong to the category of the renewal models, among which we consider the Log-normal, Gamma, Weibull, Double-exponential and Brownian Passage Time (BPT) distributions.

The comparison between these models and the Poisson model has been carried out introducing the concept of likelihood, L, of a realization of a stochastic process under a given assumption. The function L is defined as the hypothetical probability that a set of events would yield a specific outcome under a specific hypothesis.

The log-likelihood function is evaluated for both the null hypothesis (ln L_P) and the renewal hypothesis (ln L_R). Regarding the first one, described by the exponential distribution, ln L_P is defined as:

$$\ln L_P = (N-1)\ln\left(\frac{1}{T_r}\right) - \frac{t_0(N)}{T_r}$$

where N is the number of observed events, $t_0(N)$ is the occurrence time of the most remote earthquake of the sequence, and T_r is the mean inter-event time (or recurrence time).

The ln L_R of the renewal hypothesis, described by any of the renewal models, is:

$$\ln L_R = \sum_{j=1}^{N-1} \ln\left\{\frac{f(\Delta t(j))}{1 - F(t \leq \Delta t(j))}\right\} - \frac{t_0(N)}{T_r}$$

where $\Delta t(j)$ is the time difference, or inter-event time, between the j-th and the $(j+1)$-th event and $f(\Delta t)$ is the adopted Probability Density Distribution (*pdf*).

As stated above, in this study we consider five kinds of statistical distributions, i.e. the Log-normal, the Gamma, the Weibull, the Double-exponential and the BPT distributions. We report in Appendixes A.2-A.6 the main features of these distributions.

The difference between the log-likelihood for the null hypothesis and the renewal hypothesis is defined as:

$$\mathrm{d}\ln L = \ln L_R - \ln L_P .$$ (1)

A positive *dlnL* means that the sequence is better described by the renewal hypothesis than by the null hypothesis.

To take into account the effect of the uncertainties of paleoseismological data on the estimation of *dlnL* values, we have used a Monte Carlo procedure. So, we have computed the average and the standard deviation of *dlnL* from a thousand inter-event by choosing the occurrence time of each event within the limits of uncertainty provided by the observations. In this procedure it is assumed that the real occurrence time has a uniform probability distribution within such time limits.

In order to check the statistical significance of the *dlnL* results we have followed a classical procedure. It consists in finding out the confidence level by which a hypothesis can be rejected with respect to the other. According to a standard practice, we can reject one of the two hypotheses only if the confidence level is higher than 95*%.* In this test we are interested in testing if the null hypothesis of the Poisson model can be rejected in light of the available paleoseismological data for any of the observed sites. Still using a Monte Carlo procedure, we build up one thousand synthetic sequences based on the Poisson distribution for the same number of events and the same total time covered by the observed data for each fault. Then we compute the desired confidence level from the percentile corresponding to the real *dlnL* value in the synthetic distribution. It corresponds to

the probability that a value equal to or smaller than the observed *dlnL* comes by chance from casual fluctuations of a uniform random distribution (Console *et al*., 2002).

2. DATA

Sequences of events on a single structure are quite infrequent to observe because the time interval covered by historical and instrumental catalogues is often too short when compared to the average recurrence time of individual faults. Since paleoseismology can extend the record of earthquakes of the past back in time up to several millennia, it represents a great opportunity to study how seismic events recur through time and thus to provide innovative contributions to seismic hazard assessment (Figure 1).

Based on these considerations, for the present study we have used data from the Database of "Earthquake recurrence from paleoseismological data" developed in the frame of the ILP project "Earthquake Recurrence Time" (Pantosti, 2000). One of the main aims of this database is to resume the information concerning the recurrence through time of strong earthquakes occurred along seismogenic faults by means of paleoseismological study. It includes information about the analyzed sites (fault, segmentation, location, kinematics, slip rates) as well as the definition of

paleoearthquakes (type of observation for event recognition, type of dating, age, size of movement, uncertainties). The database contains prevalently

faults for which more than two dated events (one inter-event) exist.

In this work we have considered sites whose seismic sequence is composed of at least six events (except for the case of Atotsugawa, Japan, for which only five events were available). Every paleosismological site was investigated by scientists who proposed an interpretation of its seismic sequence combining the instrumental and historical earthquake records with paleoseismological study.

We have used the age of paleoevents as indicated by the authors.

For the Mediterranean area, we have extracted five sequences of earthquakes: the Fucino fault in Central Italy (Galadini and Galli, 1999), the Irpinia and the Cittanova fault in Southern Italy (Galli and Bosi, 2002; Pantosti *et al.*, 1993), the Skinos fault in Central Greece (Collier *et al.*, 1998), and El-Asnam fault in Northern Algeria (Meghraoui and Doumaz, 1996). Other paleosismological and/or historical sequences belong to *i*) Northern America: San Andreas fault Wrightwood site (Fumal *et al.*, 2002), San Andreas fault Pallet Creek site (Sieh, 1978; Biasi *et al.*, 2002) and Cascadia (Atwater and Hemphill-Haley, 1997), *ii*) New Zealand: Pakarae River fault (Ota *et al.*, 1991), Awatere fault (McCalpin, 1996), Rotoitipakau fault (Berryman *et al.*, 1998), *ii*) China: Daqingshan fault (Ran *et al.*, 2003) and Zemuhe fault (He and Ren, 2003), and *iiii*) Japan: Nankai fault, Miyagi fault, Atera fault, Tan'na fault,

Atotsugawa fault and Nagano fault (Committee for Earthquake prediction, 2001) (Figure 2). It is evident that in the sites (except for Nankai, Tan'na, and Miyagi) only the youngest events are characterized by an exact occurrence time because they are instrumental or historical; instead most of them are paleoseismological, thus their age is affected by uncertainty (Figure 2 and Table 1). In fact, dating of events depends largely on the presence of material suitable for radiometric dating in correspondence of the event horizons, and uncertainties are related both to the availability of chronological constrain in the stratigraphic sequence and to the uncertainty that affect the single radiocarbon date. In some cases the uncertainties are of the same size of the time intervals between consecutive events, so that two events have been reported within the same time limits.

4.   RESULTS AND DISCUSSION

By using the ages of paleoearthquakes with their associated uncertainties, we compared the renewal and the uniform Poisson models, taking the latter as null hypothesis. The comparison was based on the log-likelihoods of the observed sequences under each model for a number of studied sites. The renewal models considered here are the Log-normal, Gamma, Weibull, Double-exponential and BPT distributions. For the Log-normal distribution in particular, we followed two different procedures: first, the shape parameter σ is obtained from the real

sequences as a free parameter; and then it is equal to 0.4, as suggested by Wells and Coppersmith (1994).

For each of the 19 (paleoseismological or historical) earthquake sequences we computed the mean inter-event time T_r with its standard deviation (see the first column of Table 2). The errors in the mean inter-event times may appear small, compared with the large uncertainties affecting the paleoseismological datations. This circumstance may be justified taking into account that all the random occurrence times are sorted in time before computing the differences between consecutive events. In this way, negative values of inter-event times, which would produce larger standard deviations, are avoided.

For every renewal model, we computed also the shape parameter with its standard deviation and the difference *dlnL* (equation 1). The values obtained for these parameters are reported in Table 2, where each pair of columns refers to one of the renewal models separately.

We first start discussing the results for the Log-normal model. Looking at the shape parameter σ obtained from the observations (Table 2), we see that only for the Fucino fault, and for the three Japanese faults with historical data (Nankai, Atera and Tan'na), σ is close to or smaller than the standard value of 0.4 adopted by Wells and Coppersmith (1994). This means that only their seismic sequences exhibit a significantly high periodicity, while the earthquake occurrence of the other

sequences has less regularity and more casualty. The largest σ values belong to the Skinos and the Rotoitipakau sites (σ = 0.91 ± 0.25 and 0.94 ± 0.36 respectively) suggesting that these sequences follow the Poisson model in reasonable way.

Since all the *dlnL* values (Table 2) are positive, we could apparently infer that the seismic sequences are characterized by a non random behaviour. However, looking at the *dlnL* values with their uncertainties, it is easy to notice that these values are clearly higher than zero only for 7 sites (Fucino, Wrightwood, Pallet Creek, Pakarae River and the three Japanese historical sets), while for the others the errors are comparable to or larger than the respective *dlnL* values.

As said earlier in Section 2, the statistical significance of such comparisons was investigated by means of a Monte Carlo procedure. One thousand synthetic sequences were simulated under the Poisson model, and the *dlnL*s so obtained were sorted out in increasing order. Figure 3 shows the cumulative distributions of the synthetic *dlnL*s for the 19 sites of this study. For each site, the plots show the comparison between the variable-σ Log-normal distribution and the Poisson distribution.

We observe that in correspondence of the zero value of the x-axis (*dlnL*= 0) most of the plots cross a value pretty close to the center of the distribution. It means that the simulations yield approximately the same number of positive and negative results for *dlnL*. The percentage of simulations that fall below the observed *dlnL*

value indicates the level of confidence by which the null hypothesis can be rejected. Table 3 shows these results in terms of the confidence level, α, for each of the models and each of the sites of this study. Only for the Fucino site, and for two Japanese sites with historical data (Nankai and Tan'na) we can reject the null hypothesis with α >95%.

Looking at the plots for the σ = 0.4 Log-normal distribution (Figure 4) we notice that the range of the *dlnL* axis extends much more to negative values. The *dlnLs* under this more restrictive hypothesis have large uncertainties suggesting that they are significantly different from zero for most of the data. Thus, most earthquake sequences appear characterized by random occurrence of seismic events, rather than by quasi-periodical behaviour. For six sequences the *dlnL* values are negative. Although the *dlnL*s of the other sites are positive, we can reject the null hypothesis by the 95% confidence level criterion only for the two historical sequences of Nankai and Tan'na. Considering only the results from the paleoseismological data sets, we can see that the highest confidence level is obtained for the Fucino fault with a value equal to 87±19%. The evident difference between the Log-normal distribution with variable σ and that with σ = 0.4 is caused by the capacity of the former to adjust the shape parameter to the data. Thus, computing σ from the data, the shape parameter improves the performance of the renewal model with respect to the Poisson hypothesis.

Considering the Gamma distribution, from a theoretical point of view we could expect that its behaviour should not be so different from that of the variable-σ Log-normal distribution, because their *pdf*s are similar to each other and the only difference is the more or less prominent peak. Indeed, for this model, the *dlnL* values (Table 2) and the cumulative *dlnL* distributions (Figure 5) are comparable with those of the variable-σ Log-normal family. However, the confidence levels α for the Gamma model are almost constantly higher than those of the previous renewal model. Consequently, Table 3 shows that for the Gamma distribution the probability that a *dlnL* value is smaller than or equal to the observed one comes from a random distribution, is frequently larger than the same probability evaluated with the Log-normal statistical family. In spite of this slightly better performance, for the Gamma distribution the sites for which we can reject the null hypothesis with $\alpha > 95\%$ are substantially the same as those observed for the variable-σ Log-normal distribution.

Regarding the Weibull distribution, we note that when its shape parameter γ is larger than 1, the sequence of earthquakes has a quasi-periodic behaviour; instead, when $\gamma < 1$ the seismic sequence is clustered. All the earthquake sequences analysed in this study have shape parameter larger than 1 (Table 2). This points out the regular behaviour of these seismic sequences. We can draw the same conclusion also looking at the values of *dlnL*, together with their uncertainties, at least for most of the sites (Table 3). From Tables 2 and 3 the quasi-periodic behaviour of the

Fucino and Atera paleoseismological data sets, together with the Nankai and Tan'na historical data sets, is confirmed also for the Weibull model. Moreover, under this renewal model, for two more sites (Daqinshan and Atorsugawa) the confidence level by which the null hypothesis of random occurrence can be rejected is close to 95%.

Figure 6 shows plots for the comparison between the Weibull and Poisson distributions. We can clearly observe that the point $dlnL$=0 is close to the 30 percentile, i.e. the number of simulations with positive $dlnL$ is significantly larger than the number of simulations with $dlnL$<0. This circumstance supports a better performance of this model in comparison with the Log-normal and Gamma models.

The results for the Double-exponential distribution (Tables 2 and 3 and Figure 7) show a behaviour similar to those of the previous three models. In this case, unlike for the three previous models, negative values for $dlnL$ were obtained for seven paleoseismological sites, showing that the uniform Poisson model performs better than the renewal model for these sites. Table 3 displays that the null hypothesis can be rejected under the Double-exponential model for the same five sites as for the Weibull model, including Daqinshan and Atorsugawa sites for which the confidence level is close to 95%.

The BPT distribution confirms the general behaviour of the renewal models examined above. The values of the shape parameters C_v (Table 2) are close to σs of the variable-σ Log-normal distribution. In fact, their definition is pretty similar.

Under the BPT model, negative values for *dlnL* were obtained for some paleoseismological sites, but not always for the same sites as under the Double-exponential model (Table 2).

Regarding the confidence level for the rejection of the null hypothesis, the BPT model achieves a result larger than 95% for only two historical data sets (Nankai and Tan'na) (Table 3). Figure 8 shows the plots of the cumulative distribution of the *dlnL* values obtained for 1000 random sequences under the BPT model, together with the *dlnL* values of the real observations (shown by black lines).

For the BPT renewal model, we have performed a further test. For each earthquake sequence, we have built up, through a Montecarlo procedure, synthetic sequences from a BPT distribution, characterized by the same number of events and the same total time covered by the observed data. The computer code allows us to choose arbitrarily the inter-event time T_r (input) and the coefficient of variation C_v (input). For each of these synthetic distributions, the corresponding T_r (output) and C_v (output) were computed. Repeating the procedure 1000 times, we have obtained an average T_r (output) and C_v (output), which are not necessarily the same as the respective input parameters. By means of a trial and error procedure, it was easy to find which pair of input parameters T_r (input) and C_v (input) would provide the same average output values as observed from the real seismic sequence.

The results of these simulations, reported in Table 4, show (in agreement with the results published by Parsons, 2008) that both the inter-event time T_r (output) and the coefficient of variation C_v (output) are systematically smaller than the respective T_r (input) and C_v (input). We have then repeated the analysis carried out for the BPT renewal model, using T_r (input) and C_v (input) as they were the parameters estimated directly from the observations. In this way we have obtained new *dlnL* values and the relative significance levels α for all the 19 fault sites (Table 5). These results do not change the conclusions drawn directly from the real observations, though they show smaller α values for all the data sets.

As the BPT renewal model has become rather popular in the last decade, we carried out a further test assuming this model as the null hypothesis against which to compare the performance of the others. Also in this case, we used the log-likelihood criterion for performance comparison. The conclusion obtained from the results (shown in Table 6) is that the BPT distribution performs generally better than all the other models, except for the Weibull distribution.

5.   CONCLUSIONS

In this paper we tested the seismic recurrence of 19 earthquake sequences to assess their characteristics of random or regular occurrence. We faced the problem of the uncertainty inherent in the paleoseismological data, because geological expressions

of the past earthquakes are not easily discernible. Uncertainties affect the age estimates of the paleoearthquakes due to both the dating methods and the availability of dating evidence in the stratigraphic sequences. In a few cases these uncertainties may be comparable to or even larger than one seismic cycle. A rigorous statistical approach to the problem of the uncertainties in the observations of recurrence times for seismic hazard assessment has been introduced by Rhoades *et al.*, (1994) and Rhoades and Van Dissen (2003). In this study we used the Monte Carlo method for dealing with such uncertainties.

We based our analysis on the comparison between the Log-normal, Gamma, Weibull, Double-exponential and BPT distributions, and the exponential distribution. With the exception of two paleoseismological data sets (Fucino and Atera) and two historical Japanese sequences (Nankai and Tan'na), whose regularity is a statistically significant feature under most of the models considered in this study, the analyzed seismic sequences appear characterized by irregular behaviour.

The lack of regularity in the earthquake occurrence for many data sets may be explained by either inherent non-deterministic fault behaviour or interaction between different faults. Indeed, closely spaced faults are characterized by a stress field that affects each other, possibly interacting with failure triggering processes. Another possible explanation of the scarce regularity found for most of the faults considered in our study could be found in the poor reliability of the data rather than

in the fault behavior per se. An in depth study on the consequences of the scarce accuracy of the occurrence times on the results for the value of the coefficient of variation and regularity of earthquake occurrence was carried out by Sykes and Menke (2006).

As outlined by the overall picture of Figure 9, our analysis pointed out a slight superiority of the Weibull model with respect to the others, as it can fit the data with a larger *dlnL*, and a comparably small standard deviation. However, the difference is not really outstanding, even if it is clear only for high values of the recurrence time and for high values of the shape parameters.

In conclusion, the hypothesis of a regular behaviour of earthquake recurrence seems not yet sufficiently tested to justify its inclusion in an operational and practically applicable earthquake forecast system.

A.1 Exponential distribution

The *pdf* of the Exponential, or Poisson, distribution is :

$$f(x) = \frac{1}{T_r} \exp\left\{-\frac{x}{T_r}\right\}$$

where T_r is the mean of the inter-event time.

A.2 Log-normal distribution

The *pdf* of the Log-normal distribution is :

$$f(x) = \frac{1}{\sigma\sqrt{2\pi}x} \exp\left\{-\frac{\left[\ln x - \mu\right]^2}{2\sigma^2}\right\}$$

where μ and σ are the mean and standard deviation of the logarithm of the inter-event time.

The Log-normal statistical distribution has been evaluated estimating the shape parameter σ both from the data and assuming the fixed value $\sigma = 0.4$ (Wells and Coppersmith, 1994): this value describes the shape parameter of a quasi-periodic seismic sequence. The increase of σ represents the decrease of the periodicity of the seismic sequence. When $\sigma \sim 1$ earthquakes occur at random over the time. For evaluating σ from data, the following equation is used:

$$\sigma = \sum_{j=1}^{N-1} \frac{\left[\ln \Delta t(j) - \mu\right]^2}{N}.$$

A.3 Gamma distribution

The *pdf* of the Gamma distribution is:

$$f(x) = \frac{1}{\beta\Gamma(\gamma)}\left[\frac{x}{\beta}\right]^{\gamma-1} \exp\left\{-\frac{x}{\beta}\right\}$$

where $\Gamma(\gamma)$ is the Gamma function, and γ and β are the shape and the scale parameters of this statistical distribution, respectively:

$$\gamma = \left[\frac{T_r}{\sigma(\Delta t)}\right]^2, \quad \beta = \frac{\left[\sigma(\Delta t)\right]^2}{T_r}$$

where T_r and $\sigma(\Delta t)$ are the mean and the standard deviation of the inter-event times in the sample:

$$T_r = \frac{1}{N}\sum_{j=1}^{N-1}\Delta t(j), \quad \sigma(\Delta t) = \sqrt{\sum_{j=1}^{N-1}\frac{\left[\Delta t(j) - T_r\right]^2}{N}}.$$

A.4 Weibull distribution

The *pdf* of the Weibull distribution is:

$$f(x) = \frac{\gamma}{\mu}\left[\frac{x}{\mu}\right]^{\gamma-1} \exp\left\{-\left(\frac{x}{\mu}\right)^{\gamma}\right\}$$

where γ and μ are the shape and the scale parameters, respectively. In particular the scale parameter of the Weibull distribution is coincident with the mean value of the inter-event times, T_r. Instead, γ is the inverse of the coefficient of variation, or aperiodicity, defined as the ratio between the standard deviation and the mean of the observed inter-event time.

A.5 Double-exponential distribution

The *pdf* of the Double-exponential distribution is:

$$f(x) = \frac{1}{2b}\exp^{-\left|\frac{x-\mu}{b}\right|} = \begin{cases} \dfrac{1}{2b}\exp^{-\frac{(x-\mu)}{b}}, & x \geq \mu \\[2ex] \dfrac{1}{2b}\exp^{-\frac{(\mu-x)}{b}}, & x < \mu \end{cases}$$

Where b and μ are the shape and the scale parameters, respectively. These parameters are determined from a set of observations from the following relations:

$$b = \frac{\sum\limits_{i=1}^{N}|x_i - \mu|}{N} \; , \qquad \mu = Tr = \frac{\sum\limits_{i=1}^{N}x_i}{N}$$

A.6 BPT distribution

The *pdf* of the Brownian passage time (BPT) distribution is (Ellsworth *et al.*, 1999; Matthews *et al.*, 2002):

$$f(x) = \left[\frac{T_r}{2\pi C_v^2 x^3} \right]^{1\backslash 2} \exp\left\{ -\frac{[x - T_r]^2}{2C_v^2 T_r x} \right\}$$

where T_r is the mean value of the inter-event time and C_v is the coefficient of variation (or aperiodicity), defined as $C_v = \sigma / T_r$. Both T_r and σ are defined as in A.3.

References

Atwater, B.F. and E. Hemphill-Haley (1997). Recurrence intervals for great earthquakes of the past 3,500 years at Northeastern Willapa bay, Washington, *U.S. G. S. Professional Paper 1576*, 108 p.

Berryman, K.R., S. Beanland and S. Wesnousky (1998), Paleoseismicity of the Rotoitipakau Fault Zone, a complex normal fault in the Taupo Volcanic Zone, New Zealand. *New Zealand Journal of Geology & Geophysics*, 41, 449-465.

Biasi, G.P., R.J. Weldon, T.E. Fumal and G.G. Seitz (2002). Paleoseismic event dating and the conditional probability of large earthquakes on the southern San Andreas Fault, California, *Bull. Seismol. Soc. Am.*, 92, 2761-2781.

Collier, R., D. Pantosti, G. D'Addezio, P.M. De Martini, E. Masana and D. Sakellariou (1998), Paleoseismicity of the 1981 Corinth earthquake fault: seismic contribution to the extensional strain in Central Greece and implications for the seismic hazard. *J. Geophys. Res.*, 103, 30001-30019.

Console, R. (2001). Testing earthquake forecast hypothesis. *Tectonophysics*. 338, 261-268.

Console, R., D. Pantosti and G. D'Addezio (2002), Probabilistic approach to earthquake prediction. *Annals of Geophysics,* 45, 435-449.

Console, R., M. Murru and G. Falcone (2010). Retrospective forecasting of M ≥ 4.0 earthquakes in New Zealand. *P. Appl. Geophys*. 167, 693-707, DOI: 10.1007/s00024-010-0068-2.

Coordinating Committee for Earthquake Prediction (2001), Report , pp 20-21 (in Japanese).

Ellsworth, W.L., M.V. Matthews, R.M. Nadeau, S.P. Nishenko and P.A. Reasenberg (1999), A physically-based recurrence model for estimation of long-term earthquake probabilities. *U.S. Geological Survey Open-File Report*, 99- 522.

Fumal, T.E., R.J. Weldon II, G.P. Biasi, T. Dawson, G.G. Seitz, W.T. Frost and D.P. Schwartz (2002). Evidence for large earthquakes on the San Andreas fault at the Wrightwood, California, paleoseismic site: A.D. 500 to present, *Bull. Seism. Soc. Am.* , 92, 2726 -2760

Galadini, F. and P. Galli (1999), The Holocene paleoearthquakes on the 1915 Avezzano earthquake faults (Central Italy): Implications for active tectonics in Central Apennines. *Tectonophysics*, 308, 142-170.

Galli, P. and V. Bosi (2002), Paleoseismology along the Cittanova fault: Implications for the seismotectonic and earthquake recurrence in Calabria. *J. Geophys. Res*., 107, 142-170.

He, H. and J. Ren (2003), Holocene earthquakes on the Zemuhe Fault in Southwestern China, *Annals of Geophysics,* 46(5), 1035–1051.

Jackson, D.D. & Kagan, Y.Y. (1993), Reply to Nishenko and Sykes. *J. Geophys. Res*. **98**, 9917-9920 (1993).

Kagan, Y.Y. and D.D. Jackson (1991), Seismic gap hypothesis: ten years later. *J. Geophys. Res*., 96, 21419-21431.

Kagan, Y.Y. and D.D. Jackson (1995), New seismic gap hypothesis: five years later. *J. Geophys. Res*., 100, 3943-3959.

Kagan, Y.Y. and D.D. Jackson (1996), Statistical tests of VAN earthquake predictions: comments and reflections. *Geophys. Res*. *Lett*., 23, 11, 1433-1436.

Luen, B. and P.B. Stark (2008), Testing earthquake predictions, in: IMS Collections, Probability and Statistics: Essays in Honor of David A. Freedman,

Institute   of   Mathematical   Statistics,   2,   302-315.   DOI: 10.1214/193940307000000509.

Matthews, M.V., W.L. Ellsworth and P.A. Reasenberg (2002), Brownian model for recurrence earthquakes. *Bull. Seismol. Soc. Am.*, 92, 2233-2250.

McCalpin, J.P. (1996), Tectonic geomorphology and Holocene paleoseismicity of the Molesworth section of the Awatere fault, South Island, New Zealand. *New Zealand Journal of Geology and Geophysics*, 39. 33-50.

Mc Cann, W.R., S.P. Nishenko, L.R. Sykes and J. Krause (1979), Seismic gaps and plate tectonics: seismic potential for maior boundaries. *Pure Appl. Geophys.*, 117, 1082-1147.

Meghraoui, M. and F. Doumaz (1996), Earthquake induced flooding and paleoseismicity of the El Asnam, Algeria, fault-related fold. *J. Geophys. Res.*, 101, 17617-17644.

Mogi, K. (1968). Sequential occurrences of recent great earthquakes, *J. Phys. Earth*, 16, 30-60.

Nishenko, S.P. & Sykes, L.R. (1993), Comment on 'Seismic gap hypothesis: ten years after' by Y.Y. Kagan and D.D. Jackson. *J. Geophys. Res.* **98**, 9909-9916.

Ota, Y., Hull, A.G. and K.R. Berryman (1991), Coseismic uplift of Holocene marine terraces in the Pakarae River area, Eastern North Island, New Zealand. *Quaernary. Research*, 35, 331-346.

Pantosti, D. (2000), Earthquake recurrence through the time. *Proceeding of the Hokudan International Symposium and School on Active Faulting, Awaij Island, Hyogo, Japan, 17th-26th January 2000*, 363-365.

Pantosti, D., D.P. Schwartz and G. Valensise (1993), Paleoseismicity along the 1980 surface rupture of the Irpinia fault: Implications for earthquake recurrence in Southern Apennines, Italy. *J. Geophys. Res.,* 98, 6561-6577.

Parsons, T. (2008). Monte Carlo method for determining earthquake recurrence parameters from short paleoseismic catalogs: Example calculations, *J. Geophys. Res*., *109*, B03302, doi:10.1029/2007JB004998.

Parsons, T., and E.L. Geist (2009). Is there basis for preferring characteristic earthquakes over Gutenberg-Richter distributions on individual faults in probabilistic earthquake forecasting?, *Bull. Seismol. Soc. Am., 99*, 2012-2019.

Ran, Y. K., P.Z. Zhang and L.C. Chen (2003). Late Quaternary history of paleoseismic activity along the Hohhot segment of the Daqingshan piedmont fault in Hetao depression zone, North China, *Annals of Geophysics,* 46(5), 1053 –1069.

Reid, H.F. (1910). The Mechanics of the Earthquake, The California Earthquake of April 18, 1906, Report of the State Investigation Commission*,* Vol.2, Carnegie Institution of Washington, Washington, D.C.

Rhoades, D.A., R.J. Van Dissen and D.J. Dowrick (1994), On the handling of uncertainties in estimating the hazard of rupture on a fault segment. *J. Geophys. Res.*, 99, B7, 13701-13712.

Rhoades, D.A. and R.J. Van Dissen (2003), Estimates of the time-varying hazard of rupture of the Alpine Fault, New Zealand, allowing for uncertainties. *New Zealand Journal of Geology and Geophysics*, 46, 479-488.

Rong, Y., D. D. Jackson, and Y. Y. Kagan (2003), Seismic gaps and earthquakes, *J. Geophys.*

Schwartz, D.P. and K.J. Coppersmith (1984), Fault behavior and characteristic earthquakes: examples from the Wasatch and San Andreas Fault Zones. *J. Geophys. Res.*, 89, 5681-5698.

Shimazaki, K and T. Nakata (1980), Time-predictable recurrence model for large earthquakes, *Geophys. Res. Lett.*, 7, 279-282.

Sieh, K. (1978). Slip along the San Andreas fault associated with the great 1857 earthquake, *Bull. Seism. Soc. Am.*, 68, 1421-1428.

Sykes, L. R., and W. Menke (2006). Repeat times of large earthquakes: Implications for earthquake mechanics and long-term prediction, *Bull. Seism. Soc. Am.*, *96, 5*, 1569-1596, doi: 10.1785/0120050083.

Wells, D.L. and K.J. Coppersmith (1994), New empirical relationships among magnitude, rupture length, rupture width, rupture area, and surface displacement. *Bull. Seismol. Soc. Am.,* 84, 974-1002.

FIGURE CAPTIONS

Figure 1 - Distribution of events along a hypothetical seismic structure compared with the length of instrumental, historical and paleoseismological catalogues of seismicity. We may have short time window within which we observe how moderate earthquakes recurred in the past even using historical record that may span between a few centuries to a couple of millennia. Paleoseismology can extend the record of past earthquakes back in time up to several millennia representing a good opportunity to investigate how strong earthquakes recur through time.

Figure 2 - Time distribution of earthquakes for the sequences considered in this study. The most recent ages of the events of each sequence are mostly historical and indicated by single solid lines, whereas for the paleoseismic events the ages are indicated by mean ages (solid lines) and the associated uncertainties (shaded areas).

Figure 3 - Cumulative distributions of $dlnL$s for 1000 synthetic sequences obtained from the Poisson distribution compared with the observed $dlnL$s computed under a variable-σ Log-normal distribution, with its uncertainty, for each site considered in this study. The ordinate of the real $dlnL$ in the synthetic distribution gives the

probability that the observed *dlnL* comes by chance from a random distribution. The vertical lines show the observed *dlnL*s and the horizontal lines show the respective probabilities. The standard deviations and their respective probabilities are shown by dotted lines.

Figure 4 - As in Figure 3, for the comparison between the $\sigma = const$ Log-normal and the Poisson distribution.

Figure 5 - As in Figure 3, for the comparison between the Gamma and the Poisson distribution.

Figure 6 - As in Figure 3, for the comparison between the Weibull and the Poisson distribution.

Figure 7 – As in Figure 3, for the comparison between the Double-exponential and the Poisson distribution.

Figure 8 - As in Figure 3, for the comparison between the Brownian Passage Time and the Poisson distribution. Black lines show the results obtained directly from the observations, red lines show the results for the "Modified" BPT model.

Figure 9 – Mean values of the log-likelihood ratio for all the models and the data sets considered in this study, with their respective error bars.

TABLE CAPTIONS

Table 1 - Age of the events for the sites analyzed in the present study. Historical earthquakes are indicated by a single date, whereas for the paleoseimic events (except for Tan'na) the age is characterized by a more or less wide range of uncertainty.

Table 2 - Results of the studied seismic sequences for the comparison of the six distributions with the Poisson distribution. For each site it is shown: the mean inter-event time T_r, the shape parameter, and the difference of the log-likelihood between the renewal model and the Poisson distribution *dlnL.* Every value is shown with its uncertainty, except for the fixed shape parameter σ = 0.4, which comes from the literature.

Table 3 - Significance levels by which the Poisson distribution can be rejected, with their uncertainties. These values refer to different renewal models and to any of the 19 sites considered in this study.

Table 4 - Inter-event times T_r and shape parameter C_v of 1000 random simulations of sequences under the BPT model given as input, compared with the corresponding mean C_v and T_r values obtained as output.

Table 5 - Results (difference of log-likelihood between the two hypothesis, *dlnL*, and confidence level α with their uncertanties) of the comparison between the "modified" BPT and the Poisson distributions. "Modified" BPT model means that as input values, C_v(input) and T_r(input), we have entered the parameters estimated from the specific analysis carried out for the BPT model (see Table 4).

Table 6 – Results of the comparison between the performance of the BPT model with those of the other renewal models considered in this study. The second and third columns display the recurrence time and coefficient of variation of each earthquake sequence. The following pairs of columns display the shape parameters and the log-likelihood ratio for all the other renewal models assuming the BPT distribution as the null hypothesis. Positive *dlnL*s mean a better performance of the tested model with respect to the BPT model.

Table 1.

	Fucino	Irpinia	Cittanova	Skinos	El Asnam
Event 1	1915 AD	1980 AD	1783 AD	1981 AD	1980 AD
Event 2	508 AD	230 AD - 620 BC	300 - 370 AD	1295 - 1680 AD	1329 - 1630 AD
Event 3	1300 - 1500 BC	620 - 2330 AD	390 AD - 4300 BC	990 - 1390 BC	1040 - 1280 BC
Event 4	3618 – 3944 BC	2460 - 4790 BC	4060 - 10770 BC	990 - 1390 BC	90 AD - 400 BC
Event 5	5576 – 5979 BC	4790 - 6650 BC	4060 - 10770 BC	670 - 1165 BC	830 - 1256 BC
Event 6	5579 - 10729 BC	9230 - 13050 BC	10710 - 13770 BC	670 - 1165 BC	1985 - 2559 BC
Event 7					2509 - 3040 BC
Event 8					2509 - 3040 BC
Event 9					4510 - 5350 BC

	Wrightwood	Pallet Creek	Cascadia
Event 1	1857 AD	1857 AD	1700 AD
Event 2	1812 AD	1812 AD	700-1100 AD
Event 3	1647-1717 AD	1496-1599 AD	650-870 AD
Event 4	1508-1569 AD	1343-1370 AD	300-500 AD
Event 5	1448-1518 AD	1046-1113 AD	50-300 BC
Event 6	1191-1305 AD	1031-1096 AD	800-1300 BC
Event 7	1047-1181 AD	914-986 AD	1320-1500 BC
Event 8	957-1056 AD	803-868 AD	
Event 9	800-881 AD	749-775 AD	
Event 10	736-811 AD	614-666 AD	
Event 11	695-740 AD	270-430 AD	
Event 12	657-722 AD	140-350 AD	
Event 13	551-681 AD		
Event 14	407-628 AD		

	Pakarae R.	Awatere	Rotoitipakau	Daqingshan	Zemuhe
Event 1	1350 AD	1848 AD	1886 AD- 665 BC	2080-2550 BC	1850 AD
Event 2	880-1020 AD	970-770 AD	1886 AD- 665 BC	4540-5140 BC	814 AD
Event 3	250-510 AD	1050 AD-2050 BC	665-4830 BC	9180-10560 BC	1000-2200 BC
Event 4	400-600 BC	3960-4230 BC	665-4830 BC	11820-13360 BC	4217-4717 BC
Event 5	1820-2100 BC	4540-4840 BC	4830-7250 BC	14050-15970 BC	5358-12441 BC
Event 6	3420-3660 BC	6380-6660 BC	7250-8530 BC	15970-16850 BC	5358-12441 BC
Event 7	4490-5090 BC				5358-12441 BC

Event 1	Nankai	Miyagi	Atera	Tan'na	Atotsugawa	Nagano
Event 2	1947.056 AD	1978.533 AD	1586.1317 AD	1930.99 AD	1858.358 AD	1847.438 AD
Event 3	1855.064 AD	1936.925 AD	164 AD -597 BC	841 AD	1041-1739 BC	1072-423 AD
Event 4	1707.909 AD	1897.226 AD	1807-2477 BC	53 AD	2053-3279 BC	694 AD -977 BC
Event 5	1605.175 AD	1861.890 AD	4018-4461 BC	1120 BC	5387-6085 BC	433 -1148 BC
Event 6	1498.608 AD	1835.637 AD	6315-6673 BC	2580 BC	7495-8599 BC	914-3736 BC
Event 7	1361.675 AD	1793.212 AD	6319-8748 BC	3900 BC		3166-3766 BC
Event 8	1099.226 AD					3286-5232 BC
Event 9	887.736 AD					4992-6871 BC
Event 10	684.997 AD					6505-7379 BC

Table 2.

Sequence	Tr [yr]	Log-normal with σ≠const		Log- normal with σ= const		Gamma	
		σ	*dlnL*	σ	*dlnL*	γ	*dlnL*
Fucino	2017 ± 294	0.41 ± 0.27	4.0 ± 1.5	0.4	2.6 ± 2.2	11.7 ± 8.5	4.1 ± 1.6
Irpinia	2626 ± 214	0.68 ± 0.22	1.0 ± 1.2	0.4	1.3 ± 2.3	2.8 ± 2.3	1.0 ± 1.1
Cittanova	2807 ± 171	0.82 ± 0.39	0.6 ± 1.1	0.4	-0.9 ± 6.6	2.8 ± 2.1	0.76 ± 0.96
Skinos	232 ± 21	0.91 ± 0.25	0.40 ± 0.80	0.4	-0.2 ± 2.3	2.1 ± 1.7	0.59 ± 0.59
El Asnam	988 ± 35	0.76 ± 0.16	0.53 ± 0.79	0.4	-0.9 ± 2.7	2.33 ± 0.66	0.87 ± 0.69
Wrightwood	104.7 ± 4.0	0.605 ±0.062	4.73 ± 0.91	0.4	6.87 ± 0.94	2.95 ± 0.75	4.68 ± 0.80
Pallet C.	148.6 ± 4.6	0.707 ±0.055	1.85 ± 0.61	0.4	3.30 ± 0.96	2.61 ± 0.46	2.38 ± 0.51
Cascadia	518.3 ± 8.5	0.74 ± 0.25	0.7 ± 1.4	0.4	0.2 ± 3.2	3.8 ± 2.2	1.4 ± 1.2
Pakarae R.	1024 ± 28	0.563 ±0.033	1.69 ± 0.37	0.4	2.62 ± 0.33	4.30 ± 0.38	2.24 ± 0.30
Awater	1674 ± 16	0.80 ± 0.25	0.00 ± 0.56	0.4	-0.1 ± 3.9	2.1 ± 1.1	0.10 ± 0.63
Rotoitipakau	1485 ± 117	0.94 ± 0.36	0.5 ± 1.4	0.4	-2.5 ± 6.5	2.7 ± 2.2	1.0 ± 1.1
Daqingshan	2349 ± 48	0.56 ± 0.24	3.3 ± 2.1	0.4	2.9 ± 2.6	7.1 ± 8.4	3.8 ± 1.8
Zemuhe	2084 ± 226	0.73 ± 0.31	1.4 ± 1.2	0.4	0.4 ± 4.6	3.9 ± 2.2	1.9 ± 1.1
Nankai	158 ± 61	0.38	4.7	0.4	4.47	6.6	4.61
Miyagi	37.0 ± 6.6	0.2	4.8	0.4	1.98	31.18	5.27
Atera	1831 ± 132	0.47 ± 0.39	3.8 ± 2.8	0.4	1.0 ± 4.1	23 ± 27	4.2 ± 2.6
Tan'na	1166 ± 254	0.23	5.3	0.4	3.2	21	5.16
Atotsugawa	2477 ± 78	0.47 ± 0.19	2.1 ± 1.3	0.4	1.93 ± 0.73	9.2 ± 7.4	2.5 ± 1.1
Nagano	1101 ± 31	0.84 ± 0.30	0.7 ± 2.0	0.4	-2.0 ± 6.3	3.5 ± 2.8	1.5 ± 1.7

		Weibull		BPT		Double- exponential	
Sequence	Tr [yr]	γ	*dlnL*	Cv	*dlnL*	b	*dlnL*
Fucino	2017 ± 294	3. 2 ± 1.2	5.4 ± 1.8	0.35 ± 0.12	3.1 ± 5.2	521 ± 197	3.9 ± 1.8
Irpinia	2626 ± 214	1.61 ± 0.47	1.6 ± 1.4	0.66 ± 0.16	0.9 ± 3.1	1251 ± 348	-0.01 ± 1.5
Cittanova	2807 ± 171	1.59 ± 0.55	1.3 ± 1.3	0.70 ± 0.23	-0.76 ± 6.8	1522 ± 486	-0.75 ± 1.5
Skinos	232 ± 21	1.38 ± 0.45	1.07 ± 0.76	0.79 ± 0.21	0.23 ± 1.6	137 ± 33	-0.92 ± 0.99
El Asnam	988 ± 35	1.51 ± 0.21	1.74 ± 0.92	0.673 ± 0.089	0.5 ± 2.2	514 ± 83	-0.87 ± 1.1
Wrightwood	104.7 ± 4.0	1.70 ± 0.21	6.8 ± 1.0	0.595 ± 0.073	5.24 ± 0.86	49.9 ± 6.3	1.2 ± 1.4
Pallet C.	148.6 ± 4.6	1.61 ± 0.14	4.10 ± 0.66	0.626 ± 0.057	2.21 ± 0.78	77.4 ± 6.3	-0.81 ± 0.77
Cascadia	518.3 ± 8.5	1.89 ± 0.49	2.6 ± 1.3	0.56 ± 0.13	-0.2 ± 3.7	232 ± 57	0.44 ± 1.5
Pakarae R.	1024 ± 28	2.071±0.091	3.50 ± 0.30	0.484 ± 0.021	2.18 ± 0.38	408 ± 33	1.09 ± 0.49
Awater	(1674 ± 16	1.42 ± 0.38	0.5 ± 1.0	0.76 ± 0.21	0.1 ± 1.6	926 ± 235	-1.3 ± 1.3
Rotoitipakau	1485 ± 117	1.55 ± 0.53	1.8 ± 1.4	0.71 ± 0.21	-2.0 ± 6.6	810 ± 239	-0.44 ± 1.8
Daqingshan	2349 ± 48	2.5 ± 1.0	5.2 ± 2.0	0.45 ± 0.13	3.0 ± 4.4	795 ± 231	3.4 ± 1.9
Zemuhe	2084 ± 226	1.91 ± 0.52	3.1 ± 1.3	0.56 ± 0.15	-0.1 ± 6.2	916 ± 252	0.99 ± 1.3
Nankai	158 ± 61	2.57	6.26	0.389	4.9	50.85	2.68
Miyagi	37.0 ± 6.6	5.58	7.13	0.179	5.2	5.02	5.04
Atera	1831 ± 132	4.3 ± 1.7	5.9 ± 2.4	0.30 ± 0.14	1.5 ± 9.8	395 ± 154	4.7 ± 1.8
Tan'na	1166 ± 254	4.4	7.18	0.22	5.6	181.76	5.82
Atotsugawa	2477 ± 78	2.87 ± 0.78	3.6 ± 1.2	0.38 ± 0.11	2.4 ± 1.4	720 ± 213	2.3 ± 1.1
Nagano	1101 ± 31	1.8 ± 1.7	3.1 ± 2.0	0.61 ± 0.16	-2.8 ± 8.1	517 ± 143	0.54 ± 2.2

Table 3

	α (%) Logn., σ≠const	α (%) Logn., σ=const	α (%) Gamma	α (%) Weibull	α (%) BPT	α (%) Double-exp.
Fucino	97.5 ± 4.1	87 ± 19	97.4 ± 4.7	98.0 ± 3.5	94 ± 36	98.2 ± 4.0
Irpinia	73 ± 24	72 ± 22	71 ± 24	72 ± 24	70 ± 35	73 ± 21
Cittanova	62 ± 21	54 ± 36	61 ± 19	63 ± 22	46 ± 42	61 ± 21
Skinos	59 ± 21	45 ± 29	61 ± 15	60 ± 16	47 ± 33	52 ± 18
El Asnam	67 ± 17	64 ± 17	71 ± 14	73 ± 14	67 ± 27	73 ± 14
Wrightwood	75 ± 16	75 ± 18	81 ± 11	79 ± 11	80 ± 13	66 ±25
Pallet C.	37 ± 19	39 ± 18	60 ± 12	65 ± 10	37 ± 25	52 ± 11
Cascadia	54 ± 36	54 ± 30	70 ± 29	77 ± 20	32 ± 45	76 ± 21
Pakarae R.	79.1 ± 5.2	84.1 ± 3.3	85.7 ± 3.2	88.9 ± 2.3	83.5 ± 4.8	85.0 ± 5.0
Awater	47 ± 17	56 ±32	44 ± 23	45 ± 27	50 ± 27	49 ± 25
Rotoitipakau	42 ± 31	45 ± 35	48 ± 28	57 ± 28	27 ± 44	60 ± 27
Daqingshan	91 ± 20	83 ± 17	92 ± 14	94.9 ± 9.3	87 ± 33	94.6 ± 7.3
Zemuhe	82 ± 18	71 ± 28	87 ± 13	90 ± 10	55 ± 41	90 ± 10
Nankai	98.35	99.7	98.25	96.93	98.5	92.2
Miyagi	66.15	58.8	73.1	85.3	72.8	57.7
Atera	98.6 ± 8.9	68 ± 31	98.9 ± 6.0	99.2 ± 2.8	85 ± 45	99.6 ± 1.3
Tan'na	99.5	99.25	99.75	99.7	99.7	99.73
Atotsugawa	93 ± 11	81 ± 16	94.8 ± 6.7	95.6 ± 5.3	93 ±12	95.0 ± 5.3
Nagano	76 ± 43	59 ± 33	90 ± 38	92 ± 17	31 ± 46	91 ± 15

Table 4

	Tr (input) [yr]	Cv (input)	Tr (output) [yr]	Cv (output)
Fucino	2176.33	0.41	2059 ± 319	0.35 ± 0.13
Irpinia	2509.67	0.97	1989 ± 757	0.67 ± 0.25
Cittanova	2629.67	1.05	2028 ± 844	0.70 ± 0.26
Skinos	243	1.4	180 ± 153	0.79 ± 0.50
El Asnam	944.75	0.87	789 ± 234	0.67 ± 0.21
Wrightwood	118.43	0.74	103 ± 80	0.66 ± 0.41
Pallet C.	155.67	0.75	133 ± 64	0.62 ± 0.28
Cascadia	508.28	0.72	419 ± 119	0.56 ± 0.20
Pakarae R.	1015.43	0.6	866 ± 205	0.48 ± 0.16
Awater	1459.66	1.2	1072 ± 519	0.76 ± 0.29
Rotoitipakau	1505.42	1.0	1108 ± 486	0.71 ± 0.24
Daqingshan	2722.57	0.55	2303 ± 539	0.45 ± 0.15
Zemuhe	2151.13	0.7	1862 ± 463	0.56 ± 0.19
Nankai	158	0.43	149 ± 20	0.38 ± 0.11
Miyagi	37	0.25	40 ± 30	0.17 ± 0.15
Atera	1831	0.35	1745 ± 235	0.30 ± 0.11
Tan'na	1166	0.25	1152 ± 115	0.223 ± 0.083
Atotsugawa	2477	0.47	2300 ± 453	0.38 ± 0.16
Nagano	1101	0.74	952 ± 223	0.61 ± 0.19

Table 5

	Tr [yr]	Cv (input)	*dlnL*	α (%)
Fucino	2017 ± 294	0.41	1.1 ± 10	69 ± 45
Irpinia	2626 ± 214	0.97	0.5 ± 1.5	63 ± 24
Cittanova	2807 ± 171	1.05	-1.0 ± 5.3	43 ± 40
Skinos	232 ± 21	1.4	0.38 ± 0.58	52 ± 31
El Asnam	988 ± 35	0.87	0.5 ± 1.8	67 ± 24
Wrightwood	104.7 ± 4.0	0.74	4.78 ± 0.63	71 ± 12
Pallet C.	148.6 ± 4.6	0.75	2.42 ± 0.54	44 ± 17
Cascadia	518.3 ± 8.5	0.72	-0.0 ± 2.5	27 ± 44
Pakarae R.	1024 ± 28	0.6	2.05 ± 0.27	82.1 ± 3.7
Awater	1674 ± 16	1.2	-0.4 ± 1.2	42 ± 19
Rotoitipakau	1485 ± 117	1.0	-0.9 ± 3.7	35 ± 34
Daqingshan	2349 ± 48	0.55	2.0 ± 4.9	74 ± 37
Zemuhe	2084 ± 226	0.7	-0.6 ± 6.3	49 ± 41
Nankai	158 ± 61	0.43	4.65	98.15
Miyagi	37.0 ± 6.6	0.25	4.42	54.4
Atera	1831 ± 132	0.35	-5.0 ± 25	14 ± 50
Tan'na	1166 ± 254	0.25	5.3	98.4
Atotsugawa	2477 ± 78	0.47	1.7 ± 1.2	87 ± 20
Nagano	1101 ± 31	0.74	-2.2 ± 6.3	35 ± 43

Table 6

Sequence	Trm [yr]	Cv	Log-normal with σ≠ const		Log- normal, σ =const	
			σ	*dlnL*	σ	*dlnL*
Fucino	2059 ± 289	0.35 ± 0.13	0.35 ± 0.13	-0.203 ± 0.061	0.4	-1.12 ± 0.92
Irpinia	1989 ± 545	0.67 ± 0.25	0.70 ± 0.24	-0.258 ± 0.036	0.4	-0.01 ± 0.22
Cittanova	2028 ± 587	0.70 ± 0.26	0.73 ± 0.26	-0.229 ± 0.081	0.4	-0.10 ± 0.40
Skinos	180 ± 61	0.79 ± 0.29	0.79 ± 0.25	-0.286 ± 0.033	0.4	-0.31 ± 0.76
El Asnam	789 ± 172	0.67 ± 0.21	0.67 ± 0.18	-0.228 ± 0.041	0.4	-0.41 ± 0.11
Wrightwood	103 ± 12	0.59 ± 0.14	0.555 ± 0.096	-0.194 ± 0.036	0.4	1.49 ± 0.44
Pallet C.	133 ± 18	0.62 ± 0.16	0.59 ± 0.11	-0.246 ± 0.018	0.4	1.17 ± 0.16
Cascadia	419 ± 77	0.56 ± 0.20	0.56 ± 0.17	-0.265 ± 0.014	0.4	-0.23 ± 0.38
Pakarae R.	866 ± 137	0.48 ± 0.16	0.49 ± 0.15	-0.265 ± 0.049	0.4	-0.04 ± 0.62
Awater	1072 ± 341	0.76 ± 0.29	0.80 ± 0.27	-0.19 ± 0.11	0.4	-0.46 ± 0.93
Rotoitipakau	1108 ± 276	0.71 ± 0.24	0.71 ± 0.21	-0.239 ± 0.071	0.4	0.14 ± 0.38
Daqingshan	2304 ± 327	0.45 ± 0.14	0.45 ± 0.14	-0.241 ± 0.038	0.4	-0.21 ± 0.72
Zemuhe	1862 ± 357	0.56 ± 0.17	0.56 ± 0.17	-0.271 ± 0.041	0.4	0.25 ± 0.36
Nankai	149 ± 17	0.38 ± 0.11	0.38 ± 0.10	-0.212 ± 0.050	0.4	-0.9 ± 1.3
Miyagi	40.3 ± 3.4	0.173 ± 0.069	0.170 ± 0.063	-0.0543 ± 0.0060	0.4	-4.1 ± 1.8
Atera	1745 ± 210	0.30 ± 0.11	0.30 ± 0.11	-0.175 ± 0.062	0.4	-1.7 ± 1.3
Tan'na	1151 ± 114	0.223 ± 0.083	0.224 ± 0.082	-0.131 ± 0.049	0.4	-2.9 ± 1.5
Atotsugawa	2300 ± 417	0.38 ± 0.16	0.39 ± 0.16	-0.225 ± 0.082	0.4	-0.8 ± 1.1
Nagano	952 ± 163	0.61 ± 0.19	0.60 ± 0.15	-0.231 ± 0.015	0.4	-0.63 ± 0.17

			Gamma		Weibull		Double-	exponential
Sequence	Trm [yr]	Cv	γ	*dlnL*	γ	*dlnL*	b	*dlnL*
Fucino	2059 ± 289	0.35 ± 0.13	14 ± 16	-0.151 ± 0.063	3.4 ± 1.6	1.03 ± 0.27	549 ± 232	-0.82 ± 0.30
Irpinia	1989 ± 545	0.67 ± 0.25	3.7 ± 5.7	-0.203 ± 0.027	1.74 ± 0.82	0.42 ± 0.25	1033 ± 529	-1.51 ± 0.44
Cittanova	2028 ± 587	0.70 ± 0.26	3.5 ± 5.4	-0.157 ± 0.077	1.67 ± 0.81	0.43 ± 0.20	1105 ± 574	-1.55 ± 0.41
Skinos	180 ± 61	0.79 ± 0.29	2.6 ± 3.3	-0.441 ± 0.089	1.48 ± 0.69	0.06 ± 0.39	112 ± 69	-2.09 ± 0.56
El Asnam	789 ± 172	0.67 ± 0.21	3.1 ± 2.8	-0.3192 ± 0.0033	1.66 ± 0.59	0.57 ± 0.33	406 ± 165	-2.41 ± 0.51
Wrightwood	103 ± 12	0.59 ± 0.14	3.4 ± 1.8	-0.78 ± 0.20	1.78 ± 0.45	1.25 ± 0.78	46 ± 12	-3.80 ± 0.82
Pallet C.	133 ± 18	0.62 ± 0.16	3.2 ± 1.9	-0.61 ± 0.18	1.72 ± 0.47	0.97 ± 0.66	62 ± 18	-3.23 ± 0.74
Cascadia	419 ± 77	0.56 ± 0.20	4.8 ± 4.8	-0.238 ± 0.046	2.04 ± 0.82	0.74 ± 0.35	179 ± 75	-1.49 ± 0.49
Pakarae R.	866 ± 137	0.48 ± 0.16	6.3 ± 5.8	-0.214 ± 0.059	2.34 ± 0.90	0.92 ± 0.34	321 ± 126	-1.28 ± 0.42
Awater	1072 ± 341	0.76 ± 0.29	3.0 ± 4.6	-0.178 ± 0.0.70	1.54 ± 0.76	0.33 ± 0.21	639 ± 356	-1.74 ± 0.47
Rotoitipakau	1108 ± 276	0.71 ± 0.24	2.9 ± 2.7	-0.292 ± 0.027	1.60 ± 0.62	0.39 ± 0.31	(602 ± 276	-1.97 ± 0.53
Daqingshan	2304 ± 327	0.45 ± 0.14	7.2 ± 7.2	-0.217 ± 0.078	2.5 ± 1.0	0.97 ± 0.37	796 ± 307	-1.21 ± 0.44
Zemuhe	1862 ± 357	0.56 ± 0.17	4.7 ± 4.6	-0.246 ± 0.046	2.03 ± 0.80	0.72 ± 0.33	798 ± 329	-1.50 ± 0.46
Nankai	149 ± 17	0.38 ± 0.11	9.3 ± 8.4	-0.201 ± 0.074	2.9 ± 1.0	1.64 ± 0.44	44 ± 14	-1.37 ± 0.43
Miyagi	40.3 ± 3.4	0.173 ± 0.069	49 ± 36	-139 ± 505	6.9 ± 4.5	1.45 ± 0.31	5.4 ± 2.4	-0.67 ± 0.21
Atera	1745 ± 210	0.30 ± 0.11	18 ± 19	-0.15 ± 0.12	3.9 ± 1.8	1.14 ± 0.27	400 ± 165	-0.72 ± 0.29
Tan'na	1151 ± 114	0.223 ± 0.083	32 ± 30	-2.9 ± 14	5.4 ± 3.9	1.33 ± 0.20	196 ± 79	-0.56 ± 0.20
Atotsugawa	2300 ± 417	0.38 ± 0.16	14 ± 119	-0.12 ± 0.14	3.3 ± 2.9	0.73 ± 0.27	670 ± 340	-0.72 ± 0.29
Nagano	952 ± 163	0.61 ± 0.19	3.5 ± 2.6	-0.357 ± 0.085	1.79 ± 0.58	0.79 ± 0.55	446 ± 161	-2.21 ± 0.69
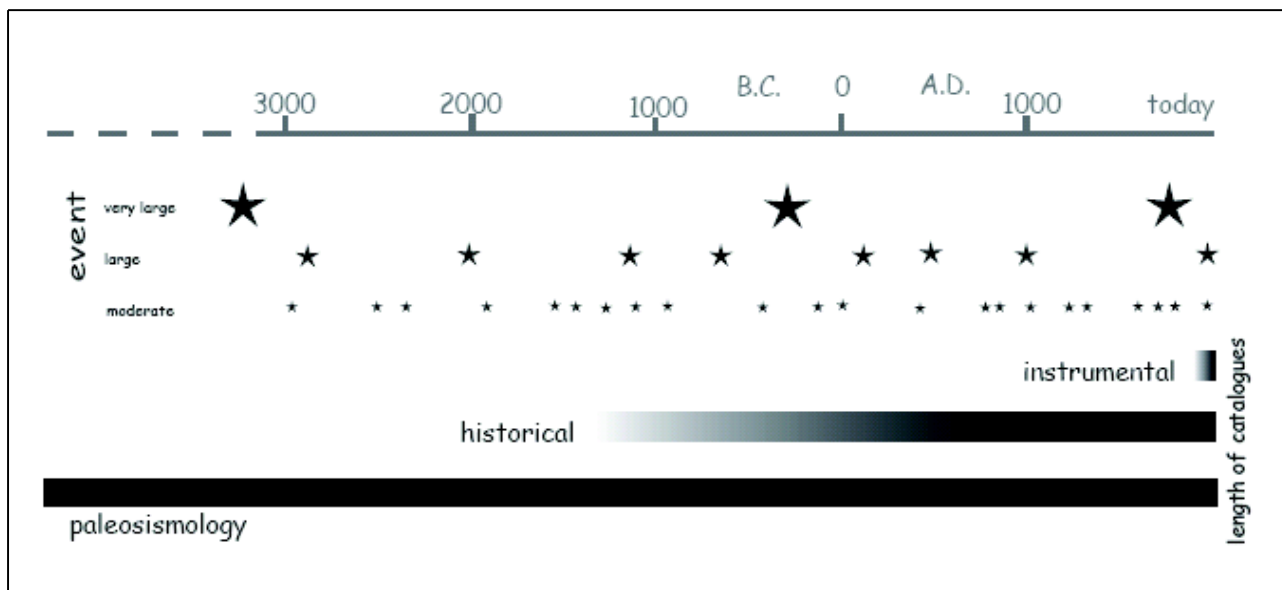
Fig. 1
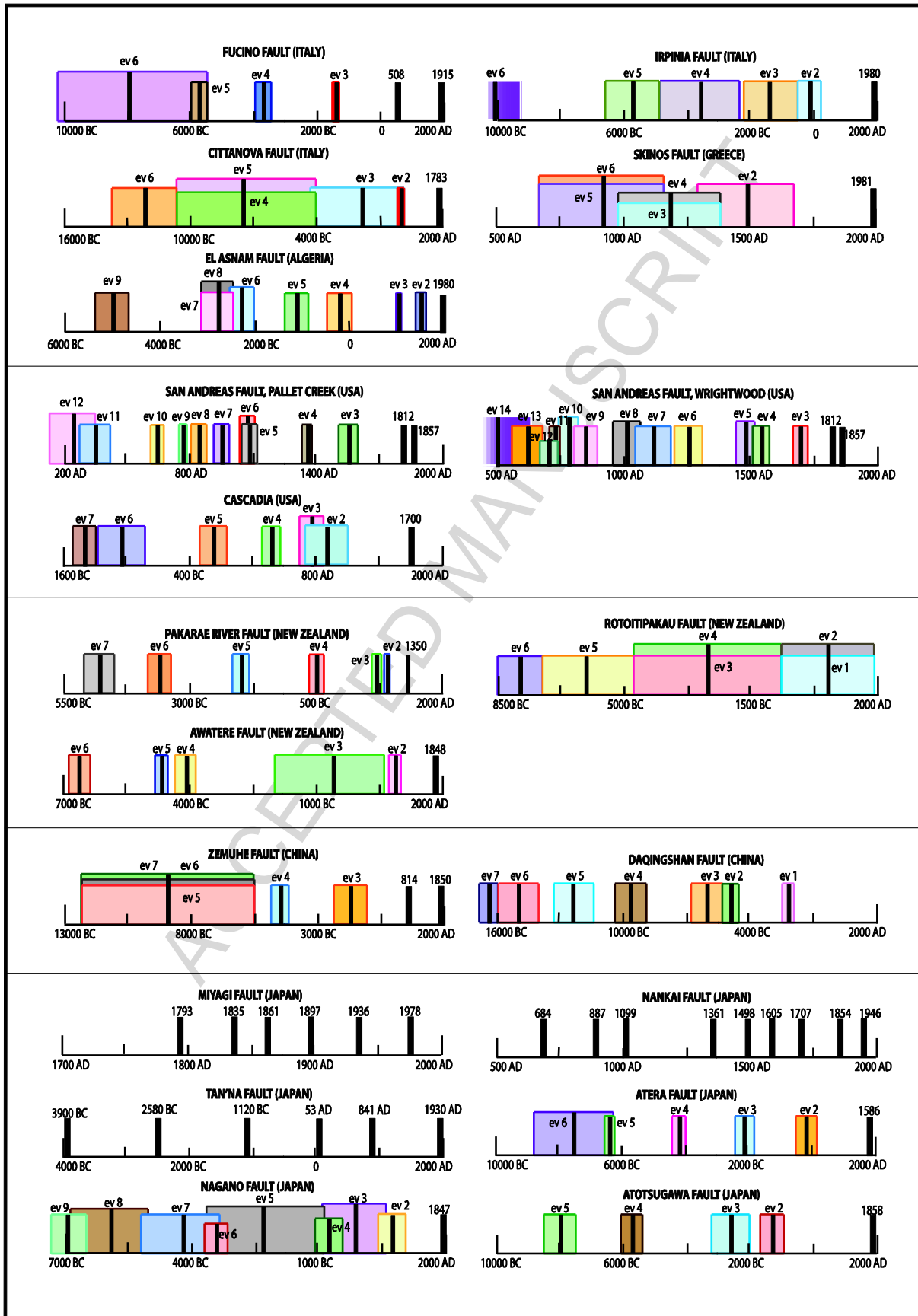
Fig. 2
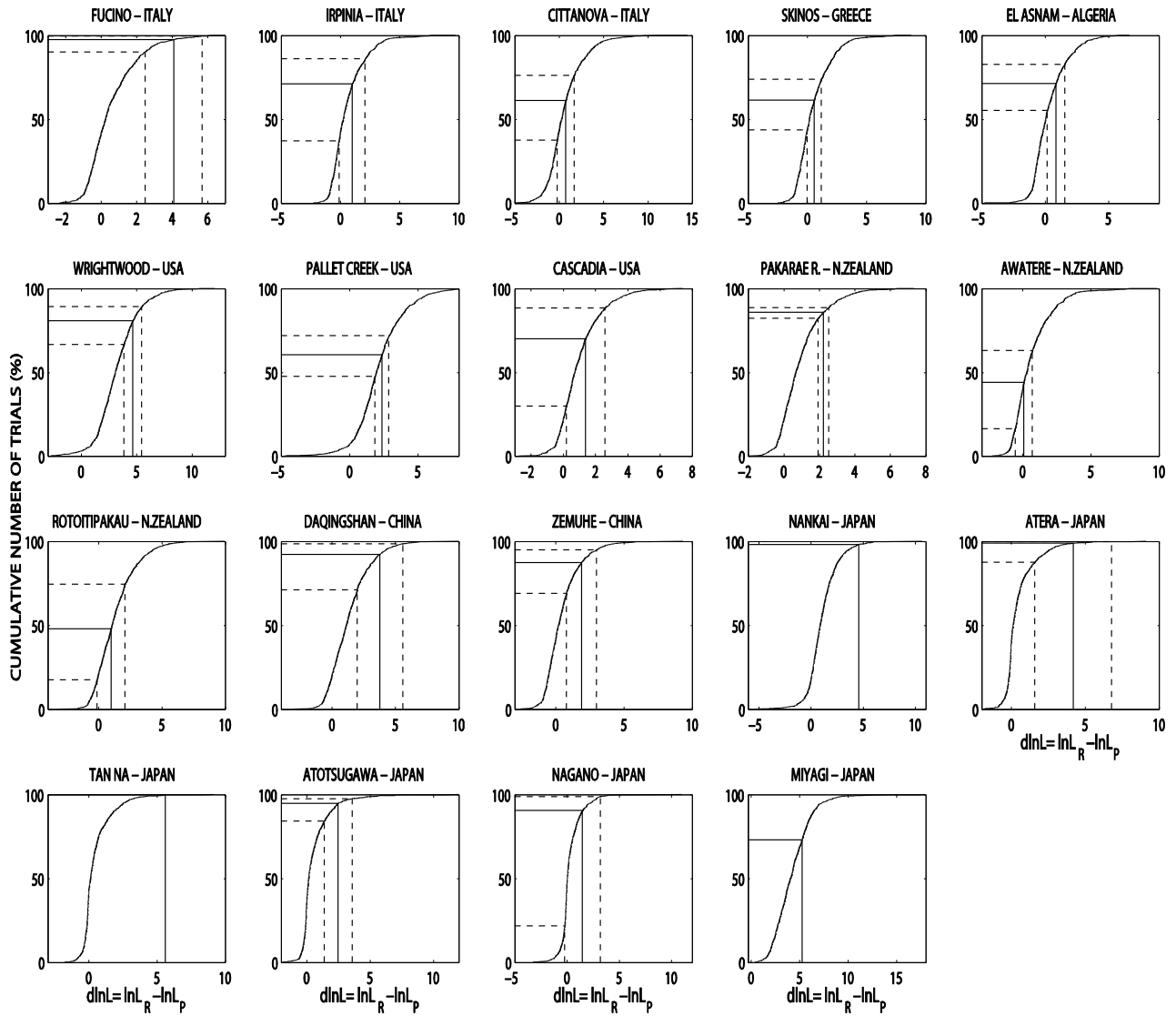
Fig. 3
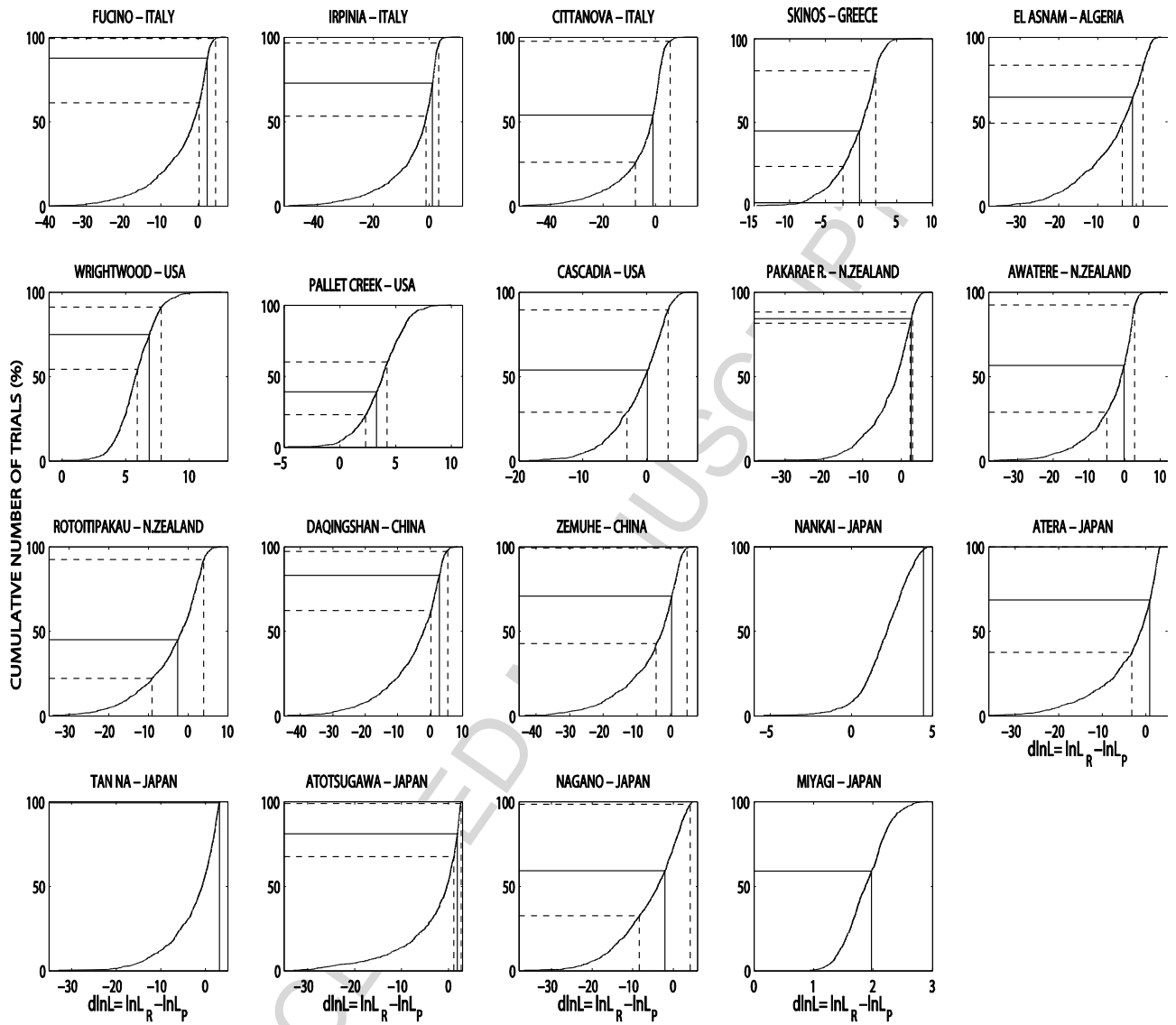
Fig. 4
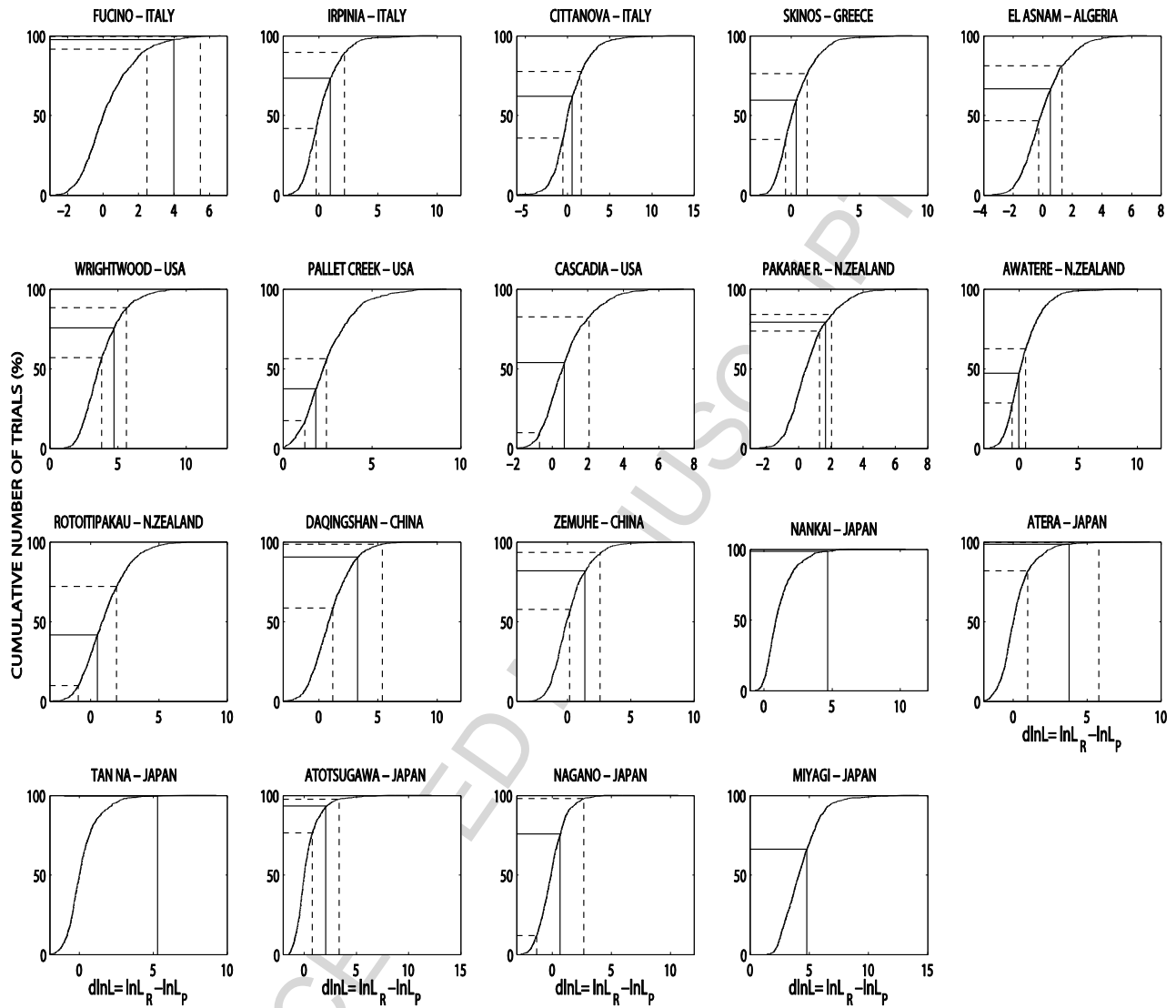
Fig. 5
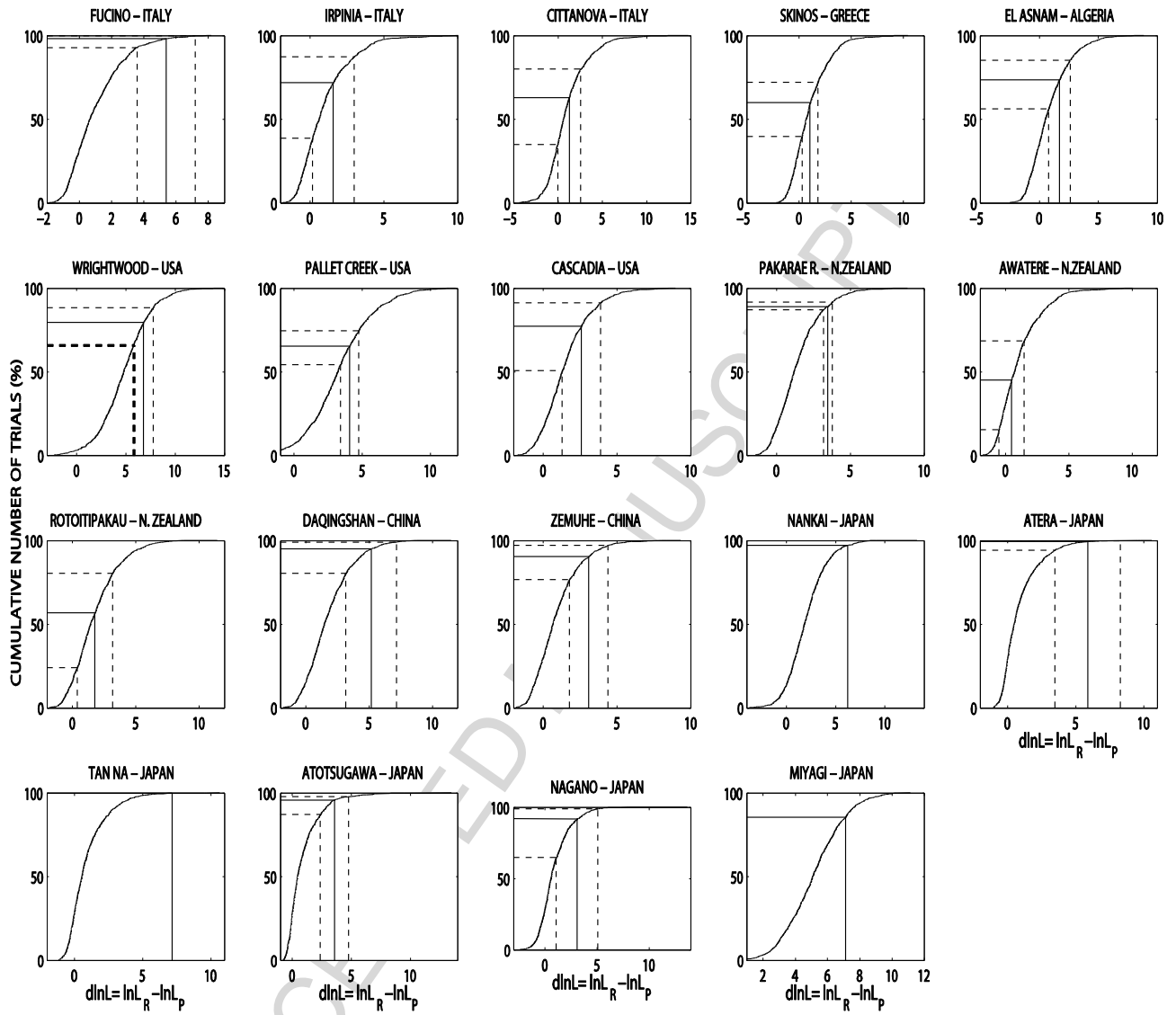
Fig. 6
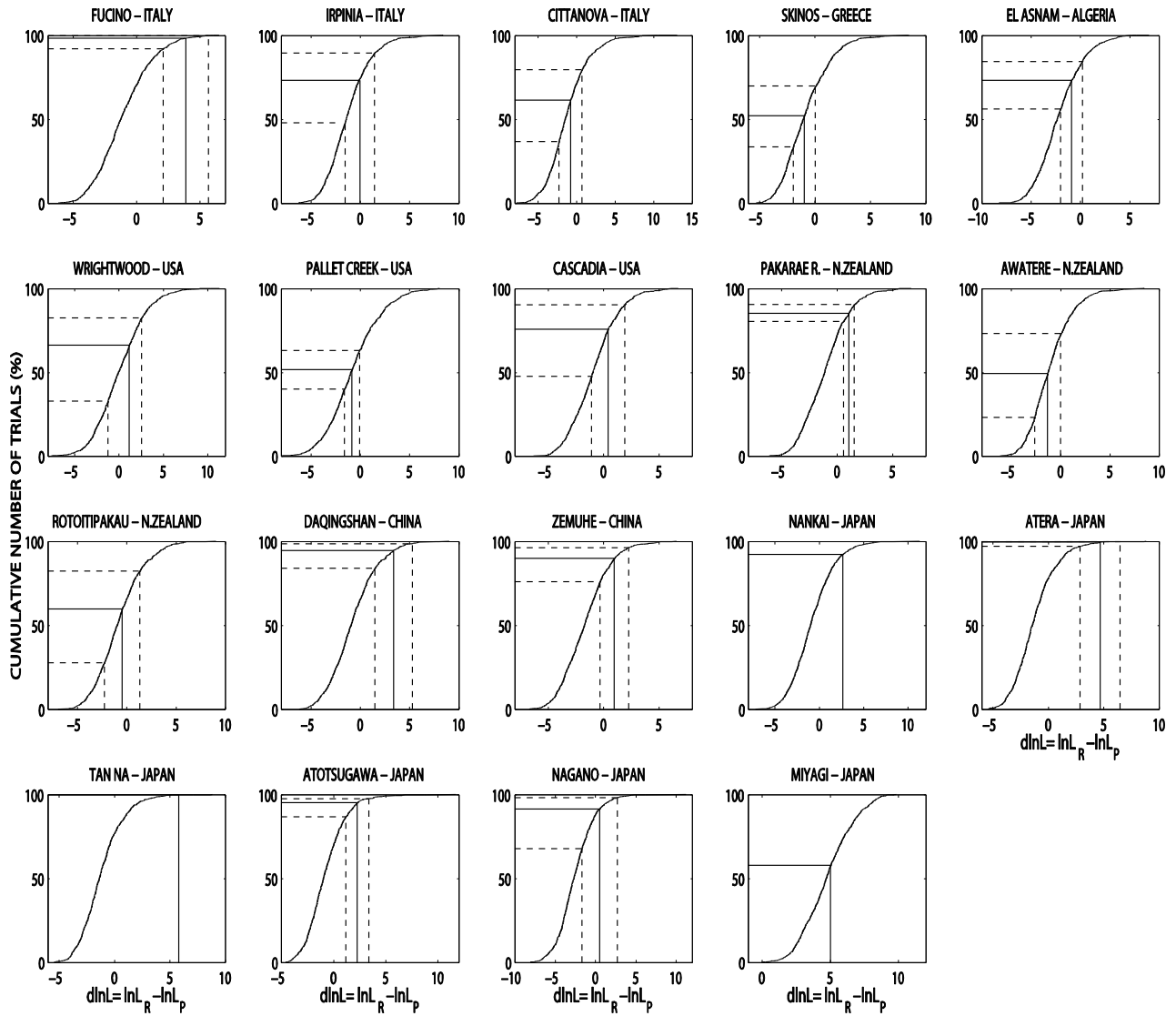
Fig. 7
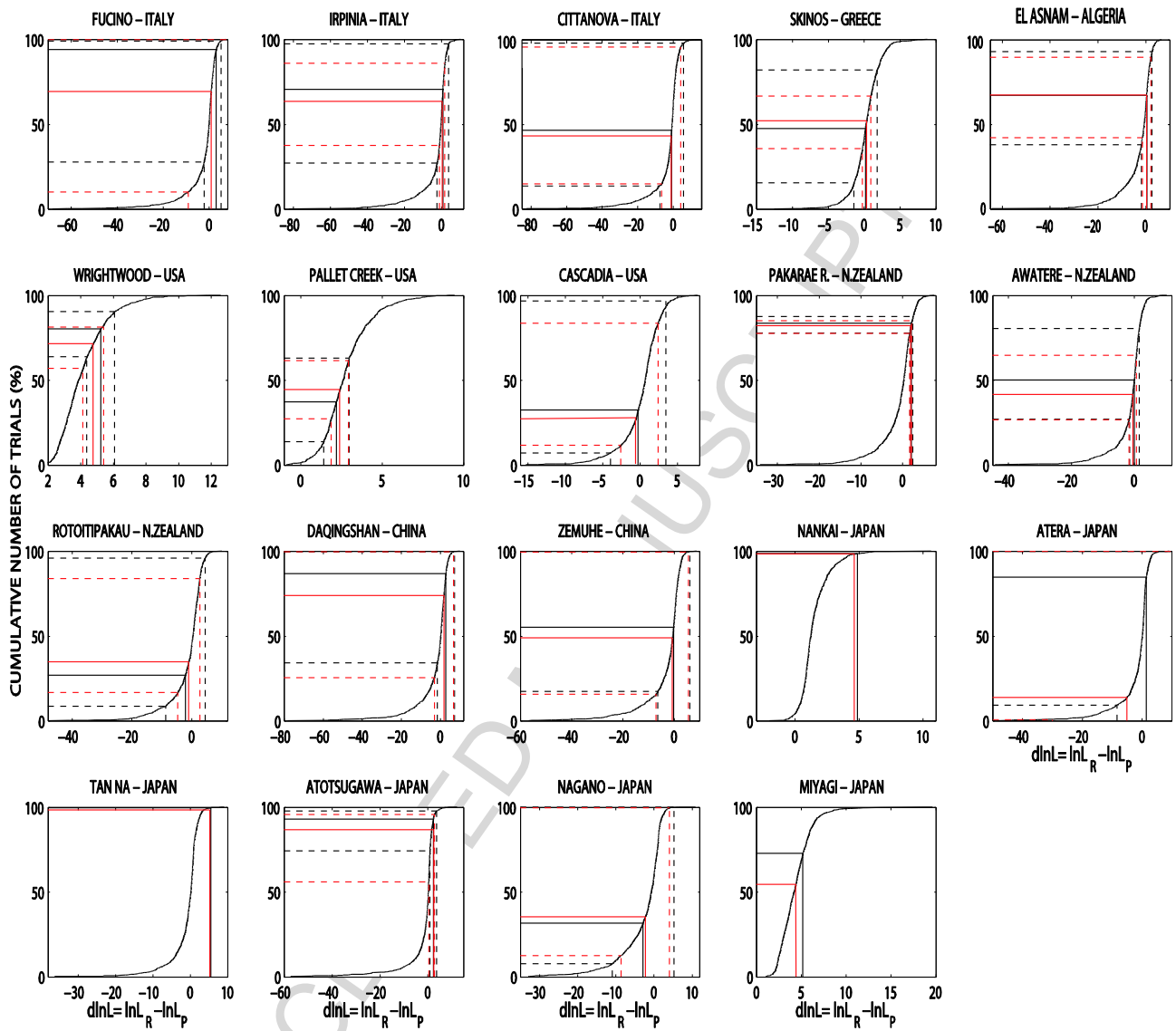
Fig. 8
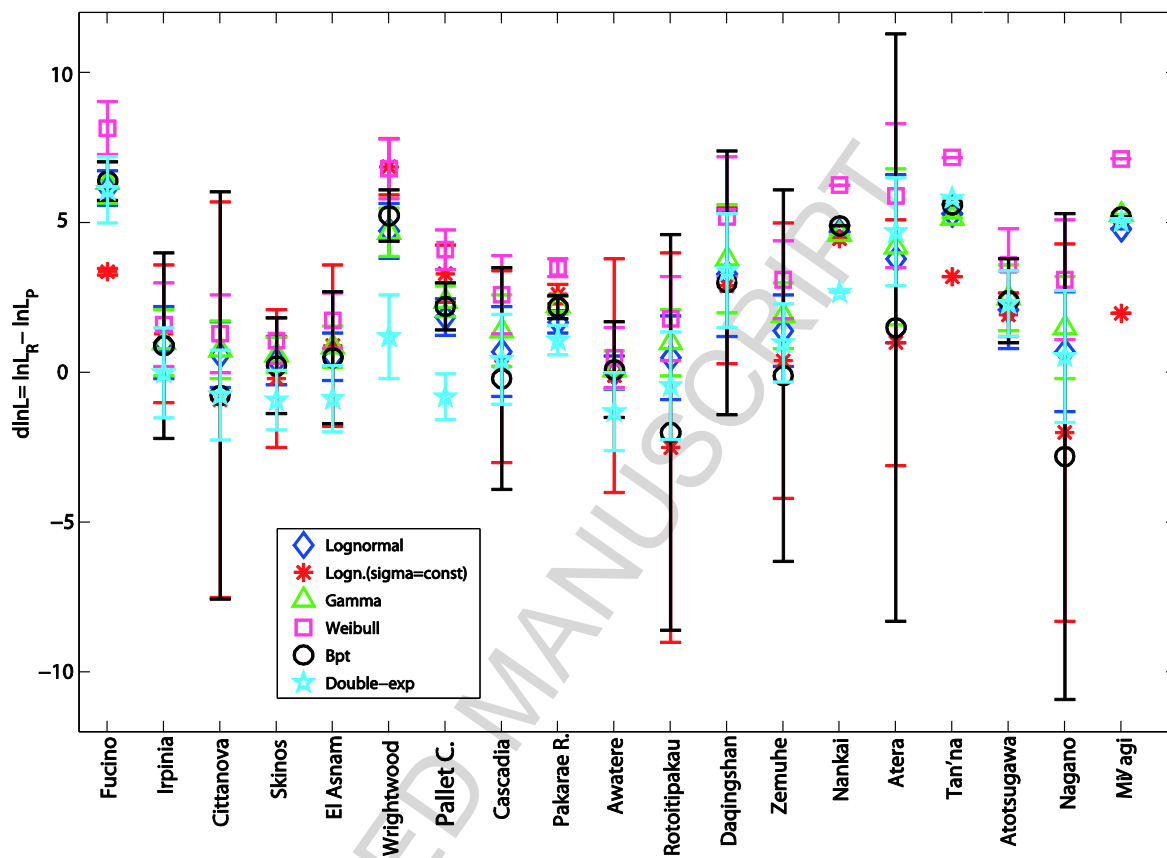
Fig. 9

Highlights

- We tested an innovative contribution to seismic hazard assessment.
- We integrated historical data with paleoseismologically dated earthquakes.
- We tested the null hypothesis using the concept of likelihood.
- We accomplished these tests for the most popular statistical models.
- We find a renewal model better than a Poisson model only for 4, out of 19 sites.